Time reversal time-domain synchronisation orthogonal frequency division multiplexing over multipath fading channels with significant tap delays

Hamada Esmaiel, Danchi Jiang

School of Engineering, University of Tasmania, Hobart, Australia
E-mail: Danchi.Jiang@utas.edu.au

Published in *The Journal of Engineering*; Received on 3rd March 2014; Accepted on 6th June 2014

Abstract: Time-reversed orthogonal frequency division multiplexing (TR-OFDM) has recently received attention as a promising spectral efficient scheme for single-input multiple-output communications over time-dispersive fading channels. For TR-OFDM, passive time reversal processing is used as a simple means for channel time dispersion reduction. In particular, pseudorandom noise (PN)-sequence padding time-domain synchronisation OFDM (TDS-OFDM) transmission scheme has been reported as an appealing alternative to the traditional cyclic prefix (CP) OFDM technology as it can provide significant improvement in the spectrum efficiency. In this study, a new correlation based coder for inter-block and inter-symbol interference removing in time-reversed TDS-OFDM, which is denoted TR-TDS-OFDM briefly is proposed. Such a coder is, then, tested for multipath channels with significant tap delays. A Zadoff–Chu sequence with perfect autocorrelation property is adopted as a training sequence (TS) for a TDS-OFDM system. Simulation results show that, by using TR-TDS-OFDM with correlation-based coder, a TS with length shorter than channel order can be used without introducing notable inter-block interference. The other merits of the proposed design are also supported by both theoretical analysis and numerical simulations.

1 Introduction

High-speed wireless communication is challenging for channels with significant multipath delays [1]. Signal propagation along multiple paths, on the one hand, introduces multipath fading, and on the other hand, gives rise to time dispersion. As the data rate increases, time dispersion becomes more pronounced and could extend over tens or even hundreds of symbol periods, leading to a dispersive impulse response. To achieve low bit error rates (BERs) in such channels, one promising approach is to use single-input multiple-output (SIMO) orthogonal frequency division multiplexing (OFDM) with multiple receiver antennas [2]. SIMO-OFDM relies on diversity combination (e.g. maximum ratio combination) to combat fading, and adopts multi-carrier (MC) transmissions (in the form of OFDM) to avoid costly channel equalisation.

Owing to its spatial and temporal focusing capability, the passive time reversal (TR) technique has been widely used in single-carrier communications for various purposes, including (but not limited to) channel equaliser simplification, multiuser interference reduction and data rate improvement among others [3]. TR was also reported as an effective means of simultaneous channel anti-dispersion and diversity combination for SIMO-OFDM [4]. In the resultant time-reversed OFDM (TR-OFDM) systems, the TR operation amounts to first convolving each of multiple received signals with the time-reversed version of its corresponding channel estimate and then combining them prior to OFDM demodulation. This operation cleverly converts multiple time-dispersive fading channels associated with SIMO-OFDM into a single channel with reduced time dispersion and less fading. As a result, a moderate cyclic prefix (CP) length can be used without introducing much inter-block-interference (IBI) even when the original channels have wide dispersion window [4]. As a by-product, it can also simplify the receiver complexity by reducing the number of required OFDM demodulators to one. TR-OFDM has been tested in various simulated and real channel environments, and demonstrated robust performance with notable bandwidth efficiency.

There are three basic types of OFDM: CP-OFDM, zero padding OFDM (ZP-OFDM) and time-domain synchronous OFDM (TDS-OFDM) [5]. The popular CP-OFDM utilises a CP as a guard interval to alleviate IBI in multipath channels [6] and it is also used to transform channel linear convolution into circular convolution, such that a finite impulse response (FIR) channel can be diagonalised by using low-complexity IFFT and FFT operation to avoid inter-symbol interference (ISI). The CP is replaced by a ZP in ZP-OFDM to tackle the channel transmission zeros problem [7]. Unlike CP-OFDM or ZP-OFDM, the TDS-OFDM adopts a known pseudorandom noise (PN) sequence as a guard interval as well as a training sequence (TS) for synchronisation and channel estimation. Consequently, it does not require any frequency-domain pilots as usual used in CP-OFDM and ZP-OFDM, leading to a better spectral and energy efficiency [8].

In this paper, it is intended to combine the TR technique for TDS-OFDM SIMO scheme with a Zadoff–Chu sequence (ZOS) sequence [9] as the TS for channel estimation, frame synchronisation, think to its perfect autocorrelation properties, as well as the guard interval for long multipath channels.

However, the cost of the spectral efficiency of TDS-OFDM is that the mutual interferences between the TS and the OFDM data block in multipath channels must be removed. In traditional systems the iterative padding subtraction (IPS) algorithm [10] is used, whereby IPS is required before the TS-based channel estimation, and demodulation are mutually conditional in conventional TDS-OFDM systems. To solve this problem, the DPN-OFDM scheme has been proposed with two repeated PN sequences [11]. The second PN sequence is not affected by the IBI) from the previous OFDM data block and hence can be used to accurate channel estimation. However, the doubled length of the guard interval in DPN-OFDM obviously compromises the spectral efficiency of TDS-OFDM, especially in long multipath fading channels. In this paper, a correlation-based coder for mutual interferences reduction is proposed. Circular convolution is used to convolve an information sequence with a perfect correlated sequence to reduce mutual interference in the TDS-OFDM.

The rest of this paper is organised as follows. Passive TR for MC communication is introduced in Section 2. In Section 3, the proposed system model is analysed. Then, the mutual interference reduction based on a correlation coder is presented in Section 4. A summary for measured time-reversal channels is discussed in Section 5. Correlation-based coder capability for system BER performance improvement is presented and discussed in Section 6. The performance is analysed and further tested in Section 7. A summary

of the major techniques and contributions of this paper is included in Section 8.

Notations: Column vectors (matrices) are denoted by boldface lower (upper) case letters; superscripts $^{\mathrm{T}}$, * and $^{\mathcal{H}}$ stand for transpose, conjugate and conjugate transpose, respectively; $\boldsymbol{I}_K$ denotes the $K \times K$ identity matrix; $\oplus$ denotes the linear convolution and $\otimes$ denotes circular convolution.

2 Passive TR for MC communication

The TR is a feedback wave focusing technique that can be used to transparently compensate for multipath dispersion in digital communications over several types of physical propagation media, such as radio or acoustic channels [12]. In a TR process, the transmitter transmits a probe at the very beginning of the communication, which is recorded at the receiver. The received probe, serving as channel information, is time reversed and retransmitted at the receiver. Thus, signal focusing can be achieved at the transmitter if the channel does not change significantly. This process can be implemented as passive TR or passive phase conjugation when a receiving array is available [13]. This paper considers a passive TR system in the multipath fading channels with significant delays such as shallow water channels, which consists of a single transducer and an M element hydrophone array.

Generally, for a signal $s(t)$ transmitted from a probe source (PS), the received signal on the ith element of a receiver array is $r_i(t) = s_i(t) \oplus c_i(t)$ in the absence of additive noise where $c_i(t)$ is the channel impulse response (CIR) and $\oplus$ denotes linear convolution. Although active TR retransmits the time-reversed version of the received signal $r_i\ (-t)$ [14–16]. Passive TR applies matched filtering at each receiver element with $c_i(-t)$ and combines them coherently.

To achieve low BERs, one promising approach is to use SIMO OFDM with multiple receiver antennas. SIMO-OFDM relies on diversity combining (e.g. maximum ratio combining) technique to combat fading, and adopts MC transmissions (in the form of OFDM) to avoid costly channel equalisation. TR-OFDM can be used for SIMO communications over time-dispersive fading channels [17]. Fig. 1 shows a TR-OFDM system. The difference between a TR-OFDM system and an SIMO-OFDM system lies in how the antenna receiver signals are processed. In conventional SIMO-OFDM, signal received by vertical line array are individually OFDM demodulated before jointing processed while in TR-OFDM they are jointly processed prior to OFDM demodulation.

The TR-OFDM was tested for CP-OFDM in [4]. In this paper, TR-OFDM tested for TDS-OFDM and solves the IBI mutual interference problem between the TS and OFDM information data block and IBI of OFDM frame on each other when guard interval is shorter than maximum channel tap delay. The TR-TDS-OFDM is tested in this paper in two cases, first one with a sufficient guard interval (TS length larger than maximum channel tap delay) and the second one with an insufficient guard interval (TS length shorter than maximum channel tap delay). The guard interval length directly impacts bandwidth efficiency spatial in the long tap delay channels [as underwater acoustic (UWA) channels] and decreasing guard interval length increase bandwidth efficiency.

3 System model

Assume the frequency-selective fading channels between the transmitter antenna and the receiver antennas to be a linear time-invariant (LTI) FIR filter [14] with impulse responses given by in the following formula [4]

$$c_m(l) = \sum_{p=0}^{L_c} c_{m,p}\delta(l-p), \quad m = 1,\ \ldots,\ M \tag{1}$$

The performance of TR communications depend entirely on the behaviour of a q-function which combines the complexity of the channel $c_m(l)$ (i.e. the number of multipaths), the number of array elements and their spatial distribution [14]. The TR channel, q assumes a perfect matched filtering that can be represented as

$$q(l) := \sum_{m=1}^{M} c_m(l) \oplus c_m^*(-l) \tag{2}$$

TR channel $q(l)$ has a time support $[-L_c,\ L_c]$ and therefore its maximum order is $L_q = 2L_c$ which doubles the $c_m(l)$'s. After passive TR, received signal $y(n)$ delayed by τ and $h(l) = q(l-\tau)$ is a delayed version of TR channels which with the same order $L_h = L_q = 2L_c$.

In TDS-OFDM, the PN TS serves not only as the guard interval of the subsequent OFDM data block, but also as the time-domain TS for synchronisation and channel estimation. Since a general PN sequence has a non-ideal autocorrelation property in conventional TDS-OFDM systems, it is not optimal for channel estimation [18]. A ZOS [19] is known to have impulsive autocorrelation function as such it can be adopted as a better TS. Given a ZOS set $\{\mathrm{e}_i^{(v)}\}$ with family size M, $v = 1, 2, 3, \ldots, M$, $i = 0, 1, 2, 3, \ldots, Q-1$, where each sequence $\mathrm{e}_i^{(v)}$ is of length Q, and each sequence element e_i is a complex number, one ZOS with Q length will have the following

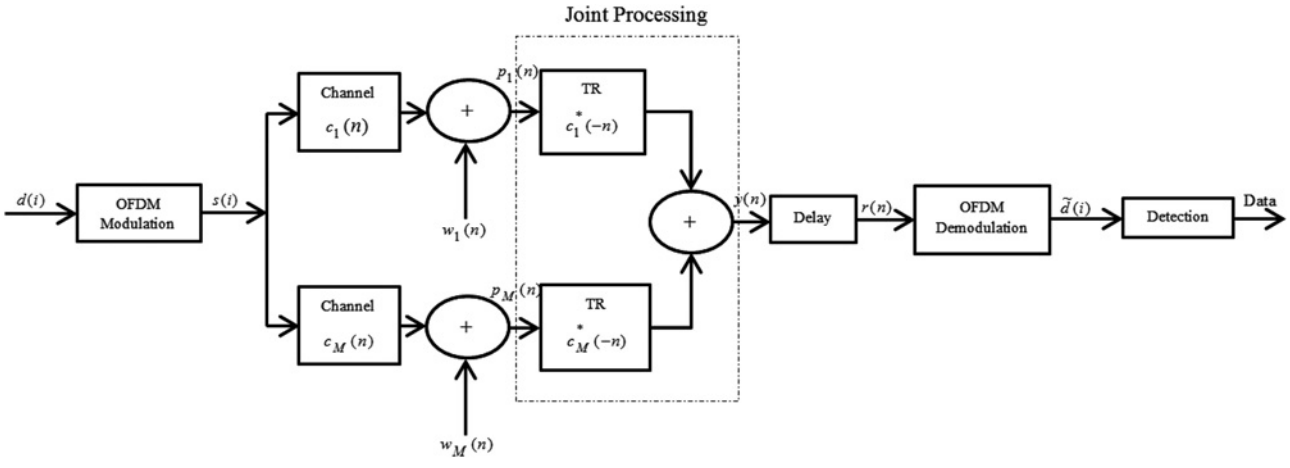

Fig. 1 *SIMO TR-OFDM system model*

doi: 10.1049/joe.2014.0064

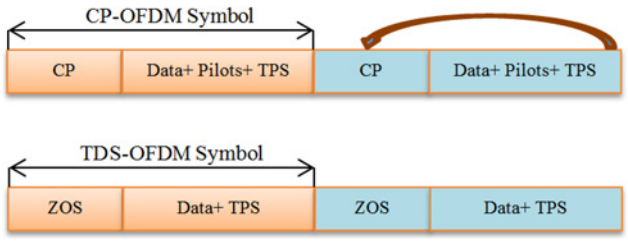

Fig. 2 *Signal structure comparison between the proposed TDS-OFDM and CP-OFDM in the time-domain*

periodic auto-correlation function (ACF)

$$R_{v,v}(\tau) = \sum_{v=0}^{Q-1} e_i^{(v)} e_{i+\tau}^{*(v)} \tag{3}$$

Here, the subscript addition $i+\tau$ is performed modulo Q and e_i^* denotes the complex conjugate of sequence element e_i. The sequence set is said to be perfectly autocorrelated if the set has the following characteristic

$$R_{vy}(\tau) = \begin{cases} Q, & \text{for } \tau = 0 \\ 0, & \text{for } \tau \neq 0 \end{cases} \tag{4}$$

The ZOS has perfect autocorrelation property, the PN sequence has good autocorrelation property, but not perfect [18], denoted by $Q[1\ (1/Q)_{1\times(Q-1)}]^{\mathrm{T}}$.

Fig. 2 shows the signal structure comparison between TDS-OFDM and CP-OFDM in the time and frequency domains. The CP used by CP-OFDM can be replaced by the known ZOS. The ith transmitted TDS-OFDM signal frame denoted by $s_i = [s_{i,0}, s_{i,1}, \ldots, s_{i,\ P-1}]^{\mathrm{T}}$ is composed of two independent parts: a known ZOS $e_i = [e_{i,0}, e_{i,1}, \ldots, e_{i,\ L-1}]^{\mathrm{T}}$ of length Q and an OFDM data block $X_i = [X_{i,0}, X_{i,1}, \ldots, X_{i,\ K-1}]^{\mathrm{T}}$ of length K

$$S_i = \begin{bmatrix} E_i \\ X_i \end{bmatrix}_{N\times 1} \tag{5}$$

where $N = Q + K$ is the length of a TDS-OFDM signal frame.

The system proposed can be illustrated in Fig. 3. The TR-TDS-OFDM transmitter employs standard TDS-OFDM modulation. K is the number of sub-carriers, Q is the guard interval (GI) length, $\boldsymbol{I}_Q$ is a $Q\times K$ guard interval matrix, $u(i) := [u(iK), \ldots, u(iK+K-1)]^{\mathrm{T}}$ is the information block and $s(i) := [s(iB), \ldots, s(iB+B-1)]^{\mathrm{T}}$ (with $B = K+Q$) the corresponding transmitted block

$$s(i) = T_e x(i) \tag{6}$$

$$x(i) = u(i) \otimes g(i) \tag{7}$$

where $\otimes$ represents the circular convolution, (7) represents the correlation-based encoder operation, g is the K-point ZOS is used in correlation-based encoder. The $Q\times K$ matrix $\boldsymbol{T}_e$ represents the operation of ZOS (TS) insertion and $u(i) = F_K^{\mathcal{H}} d(i)$, $d(i)$ is the inverse fast Fourier transform (IFFT) input and the $K\times K$ matrix $\boldsymbol{F}_K$ (with $[\boldsymbol{F}_K]_{p,q} = \left(1/\sqrt{K}\right)\exp\left(\left(-\mathrm{j}2\pi(p-1)(q-1)\right)/K\right)$ represents the K-point fast Fourier transform (FFT) operation. Let I_e be the last L_e rows of the $K\times K$ identity matrix $\boldsymbol{I}_K$.

At the TR-OFDM receiver, joint processing of $p_m(n)$ is conducted by using passive TR. Passive TR is used to focus signals in time and/or space. In the context of TR-TDS-OFDM, the TR operation amounts to generating $y(n)$ as $y(n) := \sum_{m=1}^{M} p_m(n) \oplus c_m^*(-n)$ with $\oplus$ standing for linear convolution. Owing to the channels $c_m(l)$ are LTI, $p_m(n)$ will be $p_m(n) = s(n) \oplus c_m(n) + w_m(n)$. Therefore $y(n)$ can be related to $s(n)$ in the following way

$$y(n) = \sum_{l=-L_c}^{L_c} q(l)s(n-l) + z(n) \tag{8}$$

This reveals that TR-TDS-OFDM transmission is equivalent to single-input single-output TDS-OFDM transmission over a so-termed TR channel in (2) with effective additive noise

$$z(n) := \sum_{m=1}^{M} w_m(n) \oplus c_m^*(-n) \tag{9}$$

After passive TR, $y(n)$ is delayed by τ to yield $r(n) = y(n-\tau)$,which, according (8), is given by

$$r(n) = \sum_{l=-(L_q/2)+\tau}^{(L_q/2)+\tau} h(l)s(n-l) + z(n) \tag{10}$$

where $h(l) = q(l-\tau)$ is a delayed version of TR channel with the same order $L_h = L_q = 2L_c$ and $z(n) := \sum_{m=1}^{M} w_m(n) \oplus c_m^*(\tau - n)$ (with slight abuse of notation without causing confusion).

The data model of TR-TDS-OFDM can be obtained as

$$r(i) = H_0 s(i) + H_1 s(i-1) + H_{-1} s(i+1) + \tilde{\boldsymbol{z}}(i) \tag{11}$$

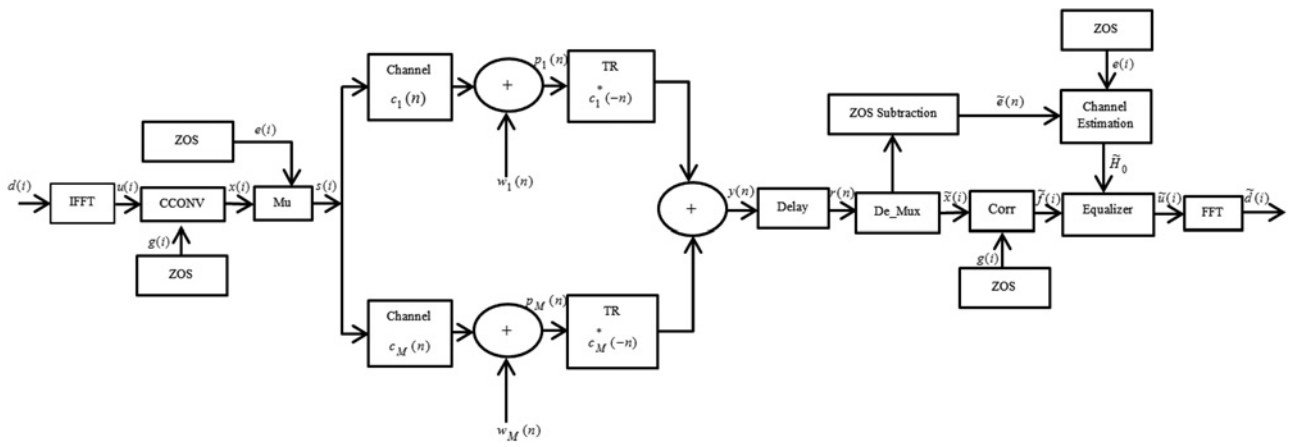

Fig. 3 *Proposed communication system*

doi: 10.1049/joe.2014.0064

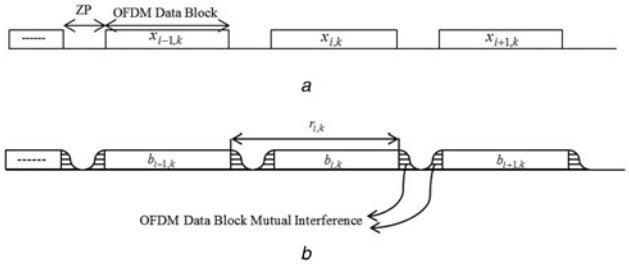

Fig. 4 *Decomposition for transmitted and received signal frames in TR-ZP-OFDM (case: channel tap delay less than guard interval)*
a ZP-OFDM transmitted signal frame
b ZP-OFDM received signal frames

Here, for $l = 0, 1, -1$, the $Q \times Q$ matrices $\boldsymbol{H}_l$ are defined to have the (p, q)th entry $[H_l]_{p,q} = h(lQ + p - q)$. $\tilde{\boldsymbol{z}}(i)$ denotes the additive Gaussian noise vector. In deriving the data model of (11), without specifying the value of guard interval relative to the TR channel order L_q. Therefore (11) is applicable for any guard interval length regardless of whether it is larger or smaller than L_q.

If a sufficient guard interval ($Q = L_h$) is used, by choosing $\tau = Q/2$ such that $h(l) = 0$ for $l < 0$ or $l > Q$, it can be verified that $H_{-1} = 0$ and $H_1 = 0$. Equation (11) becomes

$$r(i) = H_0 s(i) + \tilde{\boldsymbol{z}}(i) \tag{12}$$

The decompositions of transmitted and received signal frames are shown in Figs. 4 and 5. The ith received OFDM frame $\{r_{i,k}\}_{k=0}^{Q+K+L_c-2}$ excluding noise now consists of two overlapping parts: $\{a_{i,k}\}_{k=0}^{Q+L_c-2}$ represents the linear convolution output between the ZOS (TS) $\{e_{i,k}\}_{k=0}^{Q-1}$ and the CIR and $\{b_{i,k}\}_{k=0}^{K+L_c-2}$ denoting the convolution output between the information sequences $\{x_{i,k}\}_{k=0}^{K-1}$ and the CIR. The expressions of received frame are given by

$$r_{i,k} = y_{i,k} + \tilde{z}_{i,k} \tag{13}$$

where $y_{i,k}$, in the case of sufficient guard interval (i.e. guard interval length longer than maximum channel tap delay), can be written as

$$y_{i,k} = \begin{cases} b_{i-1,k+N} + a_{i,k} & 0 \le k < L_c - 1 \\ a_{i,k} & L_c - 1 \le k < Q - L_c + 1 \\ b_{i,k} + a_{i,k} & Q - L_c + 1 \le k < Q + L_c - 1 \\ b_{i,k} & Q + L_c - 1 \le k < Q + K - L_c + 1 \\ b_{i,k} + a_{i+1,k-N} & K + Q - L_c + 1 \le k < K + Q \end{cases} \tag{14}$$

and in the case of insufficient guard interval (guard interval length shorter than maximum channel tap delay) it can be written as (15).

Shown in Fig. 4 are the decompositions of transmitted and received frames for ZP-TR-OFDM. In the case of TR-ZP-OFDM, no IBI will be in case of guard interval length equal or longer than maximum channel tap delays, it will only present in case of insufficient guard interval length. In case of TR-TDS-OFDM, mutual IBI presents in all the cases: for sufficient guard interval length, the IBI will be between data and TS as shown in Fig. 5*d*. In the case of insufficient guard interval length, the IBI mutual interference will be between TS and data block and also between data blocks itself as shown in Fig. 5*f*. The mutual interference will effect on channel estimation accuracy and synchronisation.

4 Mutual interference reduction based on correlation coder

As illustrated in Fig. 5, the TS and the OFDM data block introduce mutual interference to each other in multipath channels. The basic principle of TDS-OFDM is that, with perfect channel information, the contribution of the TS can be completely subtracted from the received OFDM data block, and then the received TDS-OFDM symbol is essentially equivalent to a ZP-OFDM symbol, which can be converted into a CP-OFDM symbol by the classical overlapping and adding scheme to realise a low-complexity channel equalisation [20]. However, perfect channel estimation for some multipath channels is very difficult, particularly for UWA channels [1].

This paper proposes a correlation coder for mutual interference reduction, where at transmitter side as shown in Fig. 3, the IFFT output $u(i)$ convolved with ZOS $g(i)$ with circular convolution data frame with encoder process as in (7). At the receiver side, as shown in Fig. 3, after frame synchronisation and TS subtraction the OFDM data frame will be

$$\tilde{x}(i) = \begin{cases} b_{i,k} + a_{i,k} + \tilde{z}_{i,k} & Q - L_c + 1 \le k < Q + L_c - 1 \\ b_{i,k} + \tilde{z}_{i,k} & Q + L_c - 1 \le k < Q + K - L_c + 1 \\ b_{i,k} + a_{i+1,k} + \tilde{z}_{i,k} & K + Q - L_c + 1 \le k < K + Q + L_c - 1 \end{cases} \tag{16.a}$$

or (see (16.b))

based on TS length [(16.a) in sufficient TS length case or (16.b) for insufficient case]. Generally, the received OFDM data symbols can represent as

$$\tilde{x}(i) = b_{i,k} + v_{i,k} + \tilde{z}_{i,k} \tag{17}$$

The $v_{i,k}$ represent the mutual interference of ZOS TS in OFDM data frame, $\tilde{z}_{i,k}$ is the additive white Gaussian noise. Receiver directly uses the known local ZOS $g(i)$ to acquire the rough correlated OFDM data frame. The correlation-based decoder operation will be

$$\tilde{f}(i) = \frac{1}{K}\tilde{x}(i) \otimes g(i) = u(i) + v_i' + z_i' \tag{18}$$

where $v'_i = (1/K)v_i \otimes g(i)$ denotes the noise term and $z_i' = \tilde{z}_i \otimes g(i)$.

$$y_{i,k} = \begin{cases} b_{i-1,k+N} + b_{i,k} + a_{i,k} & 0 \le k < L_c - 1 \\ b_{i,k} + a_{i,k} & L_c - 1 \le k < Q + L_c - 1 \\ b_{i,k} & Q + L_c - 1 \le k < K + Q - L_c + 1 \\ b_{i,k} + a_{i+1,k} & Q + K - L_c + 1 \le k < K + 2Q - L_c + 1 \\ b_{i,k} + a_{i+1,k-N} + b_{i+1,k-N} & 2Q + K - L_c + 1 \le k < K + Q \end{cases} \tag{15}$$

$$\tilde{x}(i) = \begin{cases} b_{i,k} + a_{i,k} + \tilde{z}_{i,k} & L_c - 1 \le k < Q + L_c - 1 \\ b_{i,k} + \tilde{z}_{i,k} & Q + L_c - 1 \le k < Q + K - L_c + 1 \\ b_{i,k} + a_{i+1,k} + \tilde{z}_{i,k} & Q + K - L_c + 1 \le k < 2Q + K - L_c \\ b_{i,k} + a_{i+1,k} + b_{i+1,k-N} + \tilde{z}_{i,k} & 2Q + K - L_c + 1 \le k < K + Q \end{cases} \tag{16.b}$$

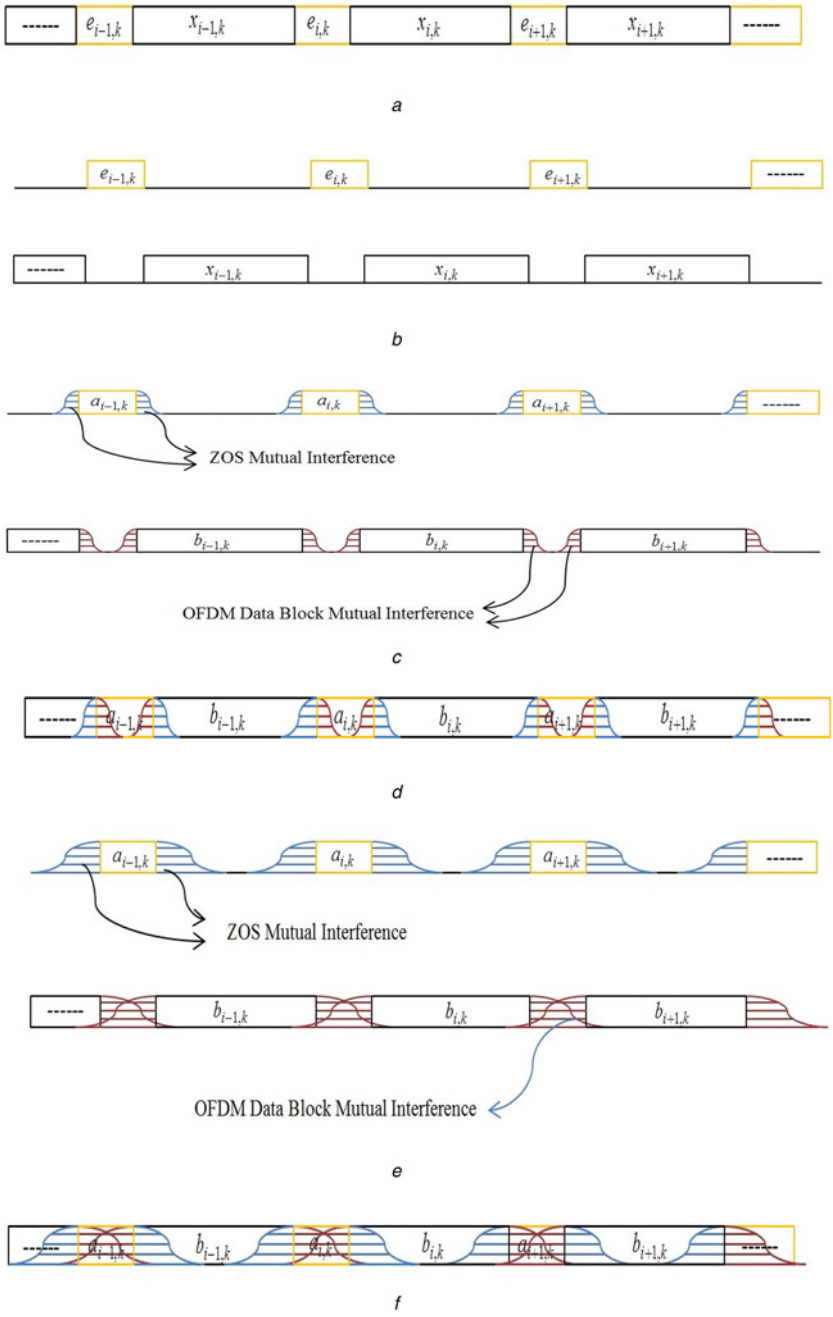

Fig. 5 *Decomposition for transmitted and received signal frames in TR-TDS-OFDM*
a Transmitted signal frame
b Time-domain decomposition for transmitted signal frame
c Time-domain decomposition for received signal frames (case: channel tap delay less than guard interval)
d Received signal frames (case: channel tap delay less than guard interval)
e Time-domain decomposition for received signal frames (case: channel tap delay greater than guard interval)
f Received signal frames (case: channel tap delay greater than guard interval)

Since the ZOS sequence $g(i)$ is independent of the OFDM data block $u(i)$, v'_i can be regarded as another noise term. The correlated-based coder reduces the mutual interference and white noise by K.

5 TR channel

In this section, the TR channel properties will be reviewed.

5.1 Realistic TR channel

An ideal TR channel offers many benefits. Whether or how much those benefits can be realised depends on how impulse-like a realistic TR channels is. To evaluate 'impulse-likeness' of a TR channel in [4] author used two different approaches for statistical approach the TR channel expressed as [4]

$$q(l)=\begin{cases}\sum\limits_{m=1}^{M}\sum\limits_{p=0}^{L_c}\left|c_{m,p}\right|^2, & l=0\\ \sum\limits_{m=1}^{M}\sum\limits_{(p,p')\in I(l)}c_{m,p}c^{*}_{m,p'}, & l\neq 0\end{cases} \tag{19}$$

where $I(l)$ denotes the set of pairs (p, p') satisfying $p-p'=l$ for p, $p'\in[0, L_c]$. The cardinality of $I(l)$ is $|I(l)|=L_c-|l|+1$.$q(l)$'s treated as deterministic number. From (19), it is observed that the terms in

doi: 10.1049/joe.2014.0064

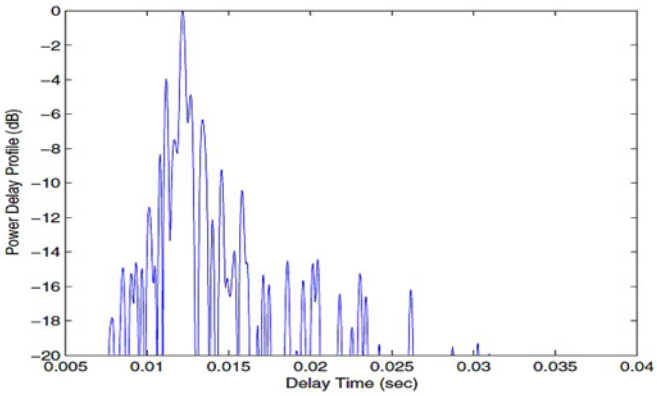

Fig. 6 *Power delay profile of measured UWA channels*

$q(0)$ are added coherently as a sum of real numbers, whereas the terms in $q(l)$, $l \neq 0$, are added up arbitrarily as a summation of complex numbers. Intuition suggests that $q(l)$, $l \neq 0$ would be suppressed and eventually become negligible relative to $q(0)$ if a sufficiently large number of terms get involved in the summations in (20). This implies that for a multipath-rich channel environment, $q_{\text{ideal}}(l)$ offers a good approximation of $q(l)$.

5.2 Measured UWA channels

Adopting the channel measurements obtained from an experimental data collection in the ASCOT01 experiment conducted off the coast of New England in June 2001, as reported in [21]. The same set of data has also been used in [4, 22, 23]. In this experiment, the source is deployed 4 m above the bottom with 103 m bottom depth. The receiver is a vertical vector sensor array with 16 receiving elements covering a depth of 30–90 m. The source–receiver range was ~10 km. To study the channels, a probe signal is repeatedly transmitted every 120 s for a period of about 160 m. The carrier frequency is centred at 3550 Hz and the bandwidth is 500 Hz. The probe signal is a linear frequency modulated (LFM) signal. By matched filtering the received signal with the LFM signal, 78 estimates of each of the 16 channels can be acquired on a large time scale of 120 s. Using the channel estimates, computing the corresponding TR channels and normalises their peak values to be one. It can be observed that (i) the mean of TR channels matches the ideal one $q_{\text{ideal}}(l)$ quite well for all M's and (ii) the variance of TR CIRs becomes smaller and smaller as M increases. This implies that the TR CIR is quite impulse-like even for a fairly small value of M (say, $M = 4$). This result is not surprising because the UWA channels are typically multipath-rich, as exemplified in Fig. 6 [4] where the power delay profile of the first channel is shown.

6 BER performance improvement using correlation-based coder

After removing mutual interference between TS and OFDM data block in TR-TDS-OFDM, it can be considered as the TR-ZP-OFDM and any equaliser used in ZP can be used in TDS. In this section, performance of the proposed system will be discussed and the effect of TS length on the BER performance will be evaluated.

The performance of the proposed TR-TDS-OFDM detector can be approximately measured by the signal-to-interference plus noise ratio (SINR)

$$\gamma(q,\ Q,\ \tau) = \frac{\text{Tr}E\left[XsX_s^{\mathcal{H}}\right]}{\text{Tr}E\left[\left(X_{\text{ISI}} + X_{\text{IBI}} + X_N\right)\left(X_{\text{ISI}} + X_{\text{IBI}} + X_N\right)^{\mathcal{H}}\right]} \tag{20}$$

where $E(\bullet)$ denotes the statistical expectation and $\text{Tr}(\bullet)$ stands for the trace of a matrix. In (20), the SINR γ has been expressed as a function of q, Q and τ to highlight its dependence on the TR channel $q := [q(-L_c),\ \ldots,\ q(L_c)]^{\text{T}}$, the TS length Q, the delay τ, X_{ISI} is the inter-symbol interference, X_{IBI} is the mutual inter-block interference and X_N are the additive white Gaussian noise.

Cast the channel taps $h(l)$'s into a vector $\boldsymbol{h} := [h(-L_h/2+\tau),\ \ldots,\ h(-Q/2),\ \ldots,\ h(0),\ \ldots,\ h(Q/2),\ \ldots,\ h(L_h/2+\tau)]^{\text{T}}$ and then split it into $h = \tilde{h} + \bar{h}$ where $\tilde{h} := [0,\ \ldots,\ 0,\ h(-Q/2),\ \ldots,\ h(0),\ \ldots,\ h(Q/2),\ 0,\ \ldots,\ 0]^{\text{T}}$ and $\bar{h} := [h(-L_h/2),\ \ldots,\ h(-Q/2-1),\ 0,\ \ldots,\ 0,\ \ldots,\ h(Q/2+1),\ 0,\ \ldots,\ h(L_h/2)]^{\text{T}}$ and collect those taps inside and outside the TS window $[-Q/2,\ Q/2]$. The inter-symbol interference X_{ISI} will be equal to zero in case of sufficient TS length and $X_{\text{ISI}} = \tilde{H}_0 S(i)$ if the guard interval length shorter than the maximum channel tap delay. X_{IBI} is the mutual inter-block interference it will be $V_{i,\ k}$ (the mutual interference between TS and OFDM data block of each frame) in case of sufficient TS length and will be $X_{\text{IBI}} = V_{i,k} + \tilde{H}_{-1} S(i+1) + \tilde{H}_1 S(i-1)$ in case of insufficient TS length.

After correlation-based coder SINR will be

$$\gamma(q,\ Q,\ \tau) = \frac{\text{Tr}E\left[FsF_s^{\mathcal{H}}\right]}{\text{Tr}E\left[\left(F_{\text{ISI}} + F_{\text{IBI}} + F_N\right)\left(F_{\text{ISI}} + F_{\text{IBI}} + F_N\right)^{\mathcal{H}}\right]} \tag{21}$$

F_{ISI}, F_{IBI} and F_N are the X_{ISI}, X_{IBI} and X_N, respectively, after reduced by K factor. Correlation-based coder increases the receiver SINR by K factor without any spectrum efficiency loss.

7 Simulation

In this section, the performance of the proposed communication system will be investigated by testing uncoded and coded BER performance of TR-OFDM via Monte Carlo simulations. In all experiment simulations, sub-carrier number $K = 1024$ and quadrature phase shift keying (QPSK) modulation are employed. To generate data symbols $d(i)$, random information bits generated are modulated directly by QPSK modulation in uncoded case, but in coded case the random information bits are first encoded by a rate-1/2 convolutional encoder with generator polynomial [65,57] [24], then the coded bits are interleaved by a block interleaver of depth 8 prior to QPSK modulation. Two different types of channels are used. One is the simulated channels where channel taps $c_m(l)$'s are generated as independent zero-mean, complex Gaussian random variables with equal variance. The other is the measured channels described in Section 5.2. The measured channels are truncated to have an order $L_c = 159$. All simulation results are averaged over 500 random realisations of simulated channels or over 78 realisations of measured channels.

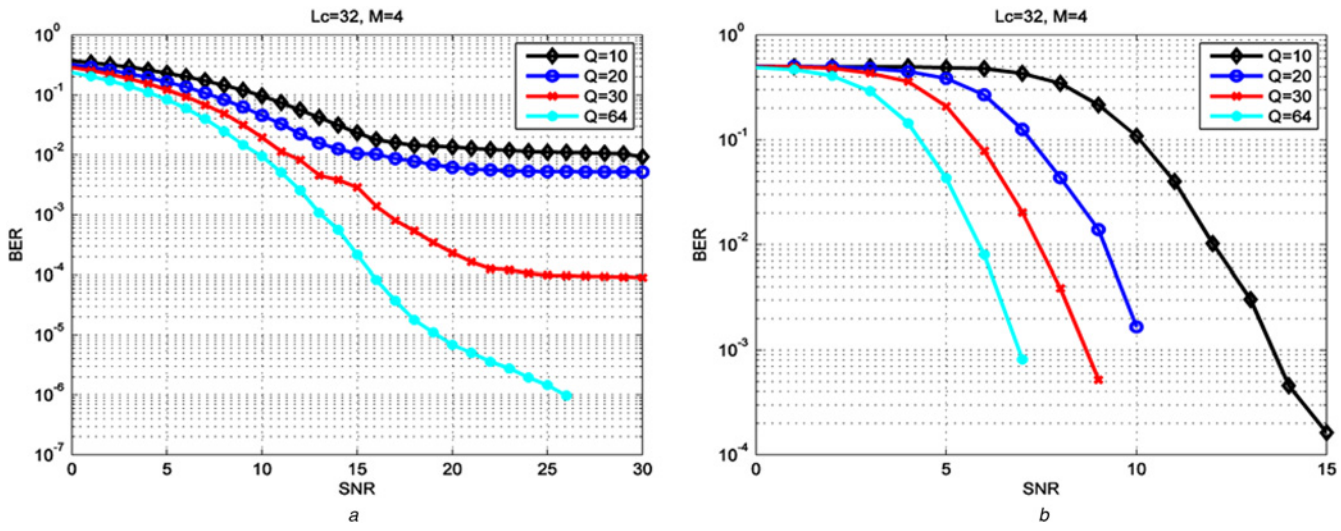

Fig. 7 *BER performance with different guard interval lengths (simulated channels)*
a Uncoded BER performance
b Coded BER performance

Channel characteristics can be estimated either frame-by-frame, using the periodically transmitted ZOS TS associated with the signal frame [10]. Channel estimated as

$$h_{0,k} = \mathrm{IFFT}\left\{\frac{\mathrm{FFT}(a_{i,k})}{\mathrm{FFT}(e_{i,k})}\right\} \tag{22}$$

Multi-tap equaliser is used to foregoing and recovery of OFDM time-domain data information $u(i)$ at low complexity by using a symbol-by-symbol detector

$$\tilde{u}(i) = \det\left(\tilde{f}(i)/\tilde{h}_0(i)\right) \tag{23}$$

Experiment 1: (*the effects of the Guard interval length*): In this experiment, the uncoded and coded BER performance of TR-TDS-OFDM with different TS lengths will be simulated. The number of receiver antennas is fixed at $M = 4$ and simulated channels of order $L_c = 32$ are generated. Channel knowledge is estimated at the receiver using (22). The uncoded performance results shown in Fig. 7*a* indicate that when the guard interval length is not sufficient (i.e. $Q = 10$, 20, 30), the BER performance tends to be saturated at high SNRs because of the residual IBI. As a result, a performance 'floor' shows up with its level decreasing as the guard interval length increases. No such error floor appears when the TS length is sufficient (i.e. $Q = 64$). In practice, the error floor can be removed by using channel coding, as confirmed by the coded BER performance results plotted in Fig. 7*b*. The same simulation is repeated for measured channels with guard interval length (i.e. $Q = 30$, 60, 90, 120, 250) and the results are plotted in Figs. 8*a* and *b*. The same observations can be made.

Experiment 2: (*the effect of the number of receiver antennas*): In this experiment, the coded and uncoded BER performance of TR-TDS-OFDM with different numbers of receiver antennas will simulate and discussed. Only simulated channels of order $L_c = 32$ are used. The TS length is fixed at $Q = 16$. The performance results are displayed in Fig. 9, showing that the performance floor

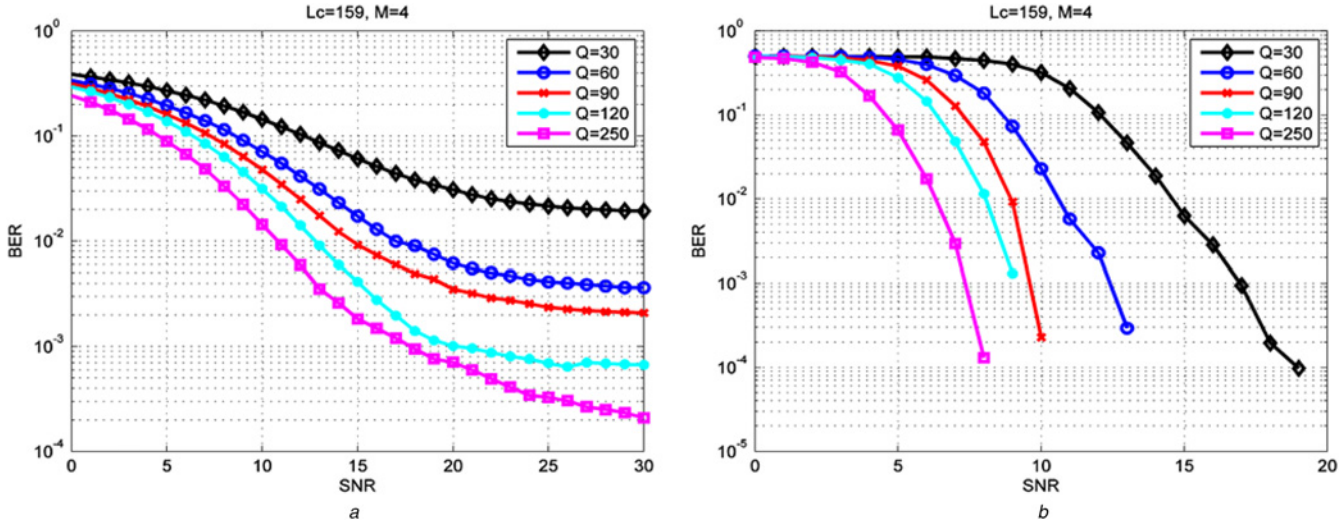

Fig. 8 *BER performance for UWA channel with different guard interval lengths (measured UWA channels)*
a Uncoded BER performance
b Coded BER performance

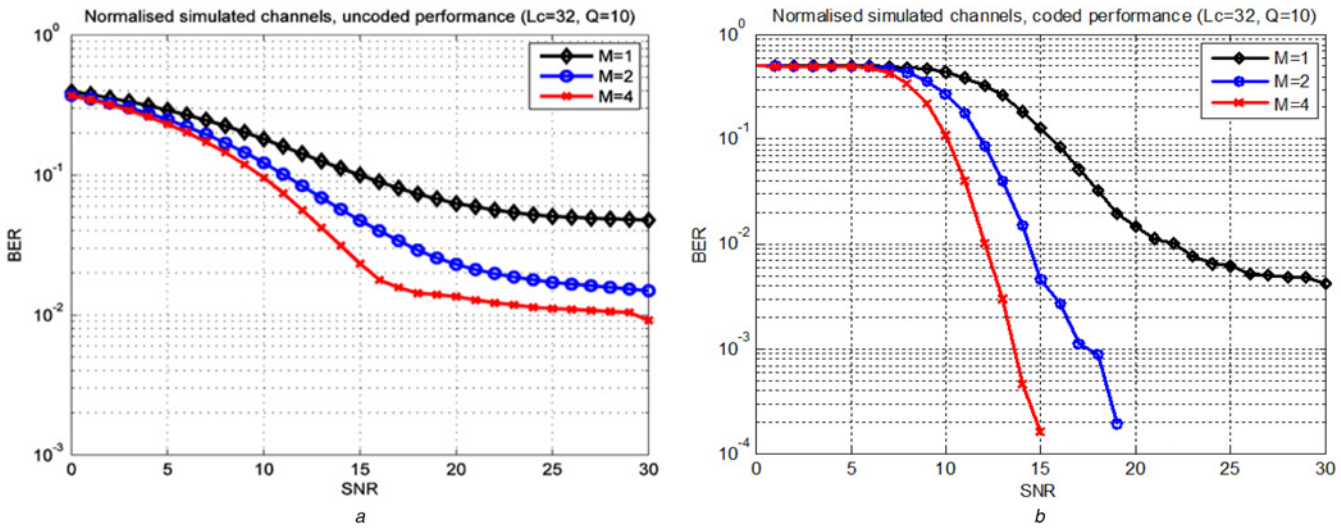

Fig. 9 *Uncoded BER performance with different number of receiver antennas M (simulated channels)*
a Uncoded BER performance
b Coded BER performance

becomes lower when the number of receiver antennas M increases. Recalling that the level of error floor is a function of the residual mutual IBI and the amount of IBI depends on how impulse-like the TR channel is, these results thus (to some extent) validate the proposed claim that the TR channel becomes more impulse-like as M increases.

Generally when the channels are rich in multipath, the TR channel is quite impulse-like even for a small M; when the channels are sparse, a large number of receiver antennas (i.e. large M) are required to render the TR channel impulse-like. These results are quite consistent with observations in the previous section. Note that for UWA channels, the same conclusion has been drawn based on waveguide physics with CP-OFDM system [22].

Experiment 3: (*performance comparison between proposed and IPS* [10]): In this experiment, the uncoded BER performance of TR-TDS-OFDM will simulate. Measured UWA channel and simulated channel with order $L_c = 32$ are used. The guard interval length is fixed at $Q = 60$ for measured UWA channel and $Q = 20$ for simulated channel. The performance results in Fig. 10 show that the performance floor becomes lower when the proposed correlation-based coder are used and it produces higher performance than conventional IPS [10] for different types of channels.

Experiment 4: (BER comparison of TR-TDS-OFDM and TR-ZP-OFDM). In this experiment, the coded and uncoded BER performance of TR-TDS-OFDM and TR-ZP-OFDM will be compared. Measured UWA channel and simulated channel with order $L_c = 32$ are used. Correlation-based coder increases the receiver SINR by K without spectrum efficiency loss. The performance results displayed in Fig. 11 compare the BER performance of TR-OFDM system for TDS and ZP guard interval. The TR-TDS-OFDM based on correlation coder produces better performance than conventional TR-ZP-OFDM. That is because the correlation-based coder not only reduces inter-block interference and inter-symbol interference, but also reduces the Gaussian channel noise by factor K.

Experiment 5: (spectral efficiency comparison of TR-TDS-OFDM and TR-ZP-OFDM): In this experiment, the effect of using TDS in spectrum efficiency is studied. If K_u is the

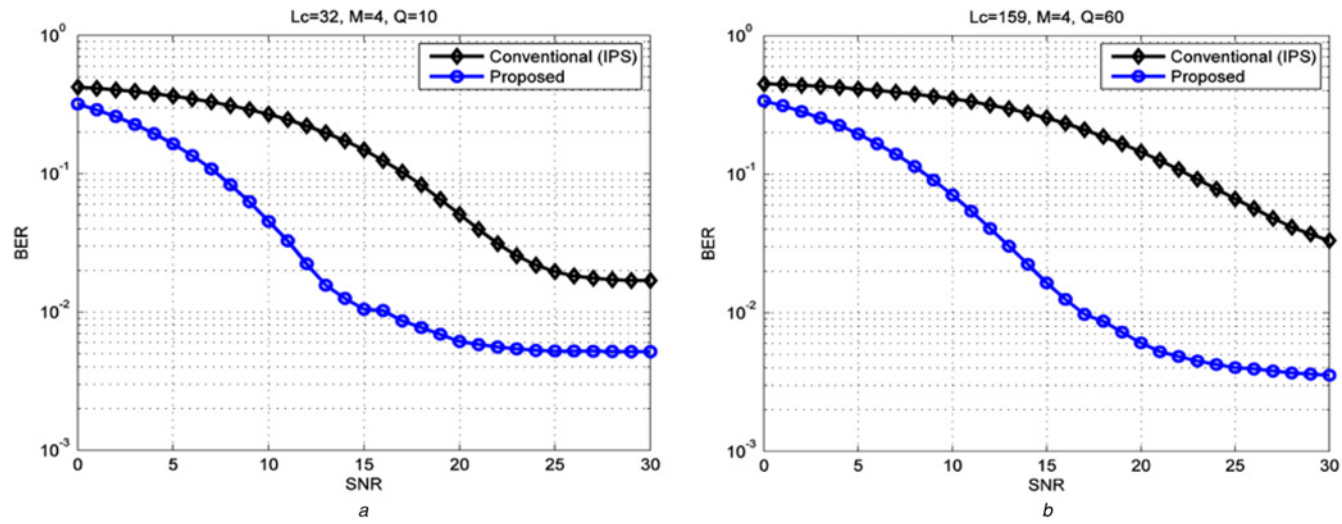

Fig. 10 *Uncoded BER performance with different mutual TR-TDS-OFDM inter-block interference reduction methods*
a Uncoded BER performance (simulated channels)
b Uncoded BER performance (measured UWA channels)

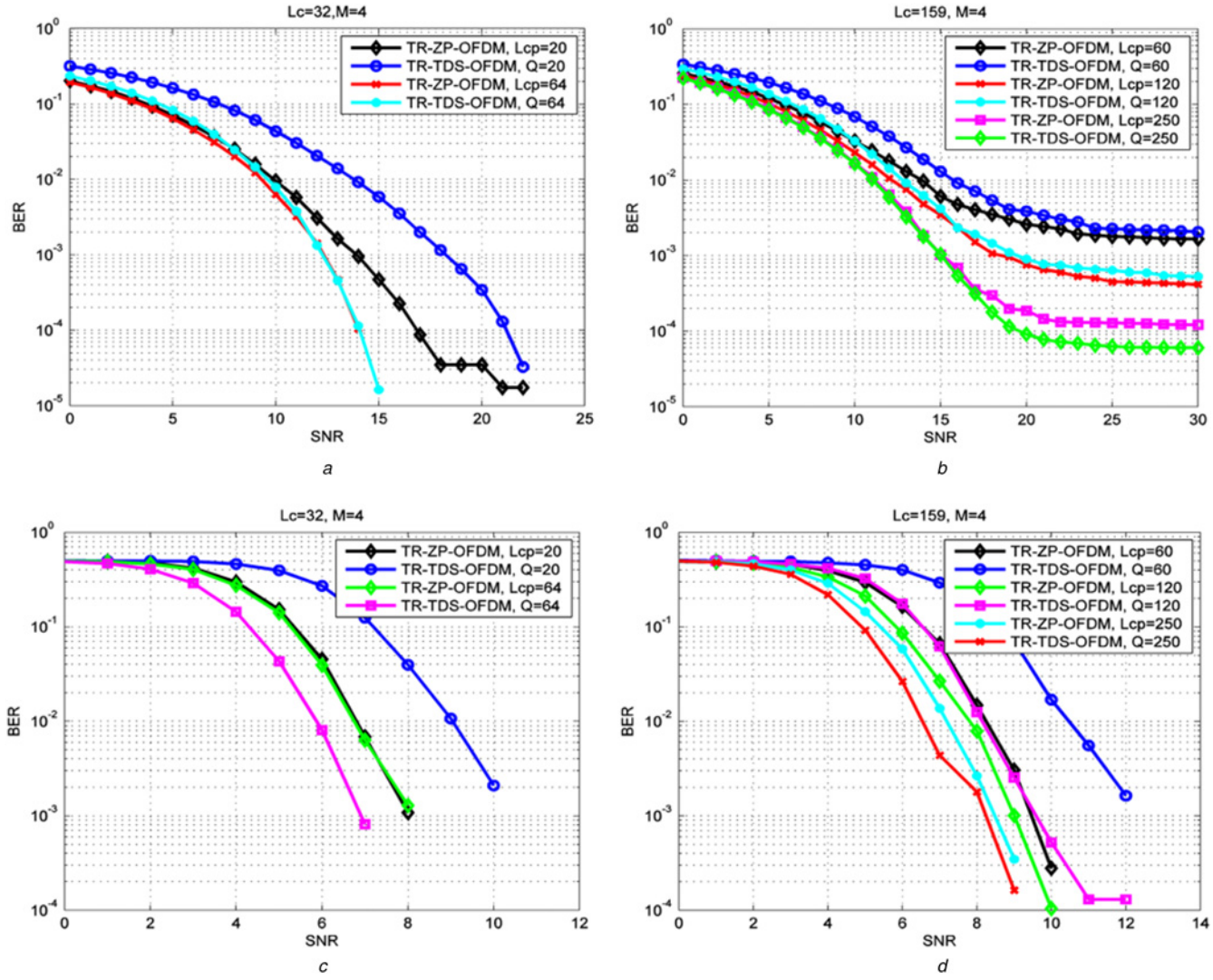

Fig. 11 *BER performance comparison between TR-ZP-OFDM and TR-TDS-OFDM*
a Uncoded BER performance (simulated channels)
b Uncoded BER performance (measured UWA channels)
c Coded BER performance (simulated channels)
d Coded BER performance (measured UWA channels)

useful sub-carrier information of TR-OFDM, the bandwidth efficiency will be

$$\eta_{\text{OFDM}} = \frac{K_u}{K + \text{GI}} \tag{24}$$

where K is the total sub-carrier and GI is the guard interval length. Note that (24) only accounts for the bandwidth efficiency loss because of the use of guard interval and pilot symbols, and its value is generally much higher than the actual one because it ignores other possible bandwidth efficiency losses because of, for example, channel coding and the use of training, etc. In TR-ZP-OFDM, 64 pilot used tones equally spaced in frequency domain to estimate the channels. Table 1 shows the comparison of the spectrum efficiency between the proposed TR-TDS-OFDM scheme and conventional TR-ZP-OFDM. It is clear that the proposed scheme offers significant spectral efficiency improvement.

Table 1 Spectral efficiency comparison

GI (length)	TR-ZP-OFDM [4], %	TR-TDS-OFDM, %
20 ($L_c = 32$)	91.95	98.08
64 ($L_c = 32$)	88.24	94.12
60 ($L_c = 159$)	88.56	94.46
120 ($L_c = 159$)	83.92	89.51
250 ($L_c = 159$)	75.35	80.38

8 Conclusion

This paper proposed a more efficient spectrum alternative to the TR-ZP-OFDM scheme. It uses correlation-based coder to enable TDS-OFDM systems to support TR schemes over long multipath fading channels such as UWA channels. A proper design of correlation-based coder is crucial to the success of TR-TDS-OFDM mutual interference reduction between TSs and information block. ZOS with perfect autocorrelation property is adopted for correlation-based coder for TS for TDS-OFDM system. In this way, not only is BER improvement achieved, but it also gives the capability of using TDS-OFDM in channels with large delay spread even if guard interval length is shorter than the maximum channel tap delay. The correlation-based coder outperforms the detector signal-to-interference plus noise ratio by a factor of K (OFDM sub-carrier number) without any spectrum

doi: 10.1049/joe.2014.0064

efficiency loss. It is shown that the proposed scheme outperforms TR-ZP-OFDM in spectrum by more than 5.7% and gives significant BER improvement. Simulation experiments are carefully conducted to test the proposed design by using simulated channels as well as real channels measured from one sea-going experiment. The experiment results also support the significant spectral and BER improvements by using the proposed scheme.

9 Acknowledgments

The authors would like to thank Professor T.C. Yang for his support with ASCOT01 experiment data. Also, we would like to thank Dr. Linglong Dai for his help and support.

10 References

[1] Esmaiel H., Jiang D.: 'Review article: multicarrier communication for underwater acoustic channel', *Int. J. Commun. Netw. Syst. Sci.*, 2013, **6**, pp. 361–376

[2] Hutter A., Hammerschmidt J., de Carvalho E., Cioffi J.: 'Receive diversity for mobile OFDM systems'. IEEE Wireless Communications and Networking Conf., 2000, pp. 707–712

[3] Hung Tuan N., Andersen J.B., Pedersen G.F.: 'The potential use of time reversal techniques in multiple element antenna systems', *IEEE Commun. Lett.*, 2005, **9**, pp. 40–42

[4] Zhiqiang L., Yang T.C.: 'On the design of cyclic prefix length for time-reversed OFDM', *IEEE Trans. Wirel. Commun.*, 2012, **11**, pp. 3723–3733

[5] Dai L., Wang J., Wang Z., Tsiaflakis P., Moonen M.: 'Spectrum- and energy-efficient OFDM based on simultaneous multi-channel reconstruction', *IEEE Trans. Signal Process.*, 2013, **61**, pp. 1–13

[6] Martin R.K., Vanbleu K., Ming D., *ET AL.*: 'Unification and evaluation of equalization structures and design algorithms for discrete multitone modulation systems', *IEEE Trans. Signal Process.*, 2005, **53**, pp. 3880–3894

[7] van Waterschoot T., Le Nir V., Duplicy J., Moonen M.: 'Analytical expressions for the power spectral density of CP-OFDM and ZP-OFDM signals', *IEEE Signal Process. Lett.*, 2010, **17**, pp. 371–374

[8] Linglong D., Zhaocheng W., Zhixing Y.: 'Time-frequency training OFDM with high spectral efficiency and reliable performance in high speed environments', *IEEE J. Sel. Areas Commun.*, 2012, **30**, pp. 695–707

[9] Jingbo M., Guihua K.: 'A novel OFDM synchronization algorithm based on CAZAC sequence'. Int. Conf. Computer Application and System Modeling, 2010, pp. V14-634–V14-637

[10] Jun W., Zhi-Xing Y., Chang-Yong P., Jian S., Lin Y.: 'Iterative padding subtraction of the PN sequence for the TDS-OFDM over broadcast channels', *IEEE Trans. Consum. Electron.*, 2005, **51**, pp. 1148–1152

[11] Jian F., Jun W., Jian S., Chang-Yong P., Zhi-Xing Y.: 'A simplified equalization method for dual PN-sequence padding TDS-OFDM systems', *IEEE Trans. Broadcast.*, 2008, **54**, pp. 825–830

[12] Gomes J., Barroso V.: 'Time-reversed OFDM communication in underwater channels'. IEEE Fifth Workshop on Signal Processing Advances in Wireless Communications, 2004, pp. 626–630

[13] Aijun S., Badiey M., Newhall A.E., Lynch J.F., DeFerrari H.A., Katsnelson B.G.: 'Passive time reversal acoustic communications through shallow-water internal waves', *IEEE J. Ocean. Eng.*, 2010, **35**, pp. 756–765

[14] Song H.C., Hodgkiss W.S., Kuperman W.A., Akal T., Stevenson M.: 'Multiuser communications using passive time reversal', *IEEE J. Ocean. Eng.*, 2007, **32**, pp. 915–926

[15] Murugan S.S., Natarajan V.: 'Performance analysis of signal to noise ratio and bit error rate for multiuser using passive time reversal technique in underwater communication'. Int. Conf. Wireless Communication and Sensor Computing, 2010, pp. 1–4

[16] Shimura T., Ochi H., Watanabe Y., Hattori T.: 'Time-reversal communication in deep ocean results of recent experiments'. Workshop on Scientific Use of Submarine Cables and Related Technologies, 2011, pp. 1–5

[17] Zhiqiang L., Yang T.C.: 'Time reversal multicarrier communications over long multipath fading channels'. Military Communications Conf., 2012, pp. 1–6

[18] Linglong D., Zhaocheng W., Jun W., Zhixing Y.: 'Joint time-frequency channel estimation for time domain synchronous OFDM systems', *IEEE Trans. Broadcast.*, 2013, **59**, pp. 168–173

[19] Jae Won K., Younghoon W., Byung Hoon K., Kwang Soon K.: 'Generalized cross-correlation properties of chu sequences', *IEEE Trans. Inf. Theory*, 2012, **58**, pp. 438–444

[20] Linglong D., Zhaocheng W., Sheng C.: 'A novel uplink multiple access scheme based on TDS-FDMA', *IEEE Trans. Wirel. Commun.*, 2011, **10**, pp. 757–761

[21] Yang T.C.: 'Temporal resolutions of time-reversal and passive-phase conjugation for underwater acoustic communications', *IEEE J. Ocean. Eng.*, 2003, **28**, pp. 229–245

[22] Yang T.C.: 'Correlation-based decision-feedback equalizer for underwater acoustic communications', *IEEE J. Ocean. Eng.*, 2005, **30**, pp. 865–880

[23] Yang T.C.: 'Measurements of spatial coherence, beamforming gain and diversity gain for underwater acoustic communications'. OCEANS, 2005, vol. **1**, pp. 268–272

[24] Wicker S.B.: 'Error control systems for digital communication and storage' (Prentice-Hall, Englewood Cliffs, 1995), vol. **1**